Tellus
SERIES A
DYNAMIC
METEOROLOGY
AND OCEANOGRAPHY
PUBLISHED BY THE INTERNATIONAL METEOROLOGICAL INSTITUTE IN STOCKHOLM

Tellus (2010), 62A, 516–529
Printed in Singapore. All rights reserved

TELLUS

The mid-depth circulation of the Nordic Seas derived from profiling float observations

By G. VOET[1]*, D. QUADFASEL[1], K. A. MORK[2] and H. SØILAND[2], [1]*Institut für Meereskunde, KlimaCampus, University of Hamburg, Bundesstr. 53, 20146 Hamburg, Germany;* [2]*Institute of Marine Research and Bjerknes Centre for Climate Research, Bergen, Norway*

(Manuscript received 10 July 2009; in final form 10 March 2010)

ABSTRACT

The trajectories of 61 profiling Argo floats deployed at mid-depth in the Nordic Seas—the Greenland, Lofoten and Norwegian Basins and the Iceland Plateau—between 2001 and 2009 are analysed to determine the pattern, strength and variability of the regional circulation. The mid-depth circulation is strongly coupled with the structure of the bottom topography of the four major basins and of the Nordic Seas as a whole. It is cyclonic, both on the large-scale and on the basin scale, with weak flow ($<1\,\mathrm{cm\,s^{-1}}$) in the interior of the basins and somewhat stronger flow (up to $5\,\mathrm{cm\,s^{-1}}$) at their rims. Only few floats moved from one basin to another, indicating that the internal recirculation within the basins is by far dominating the larger-scale exchanges. The seasonal variability of the mid-depth flow ranges from less than $1\,\mathrm{cm\,s^{-1}}$ over the Iceland Plateau to more than $4\,\mathrm{cm\,s^{-1}}$ in the Greenland Basin. These velocities translate into internal gyre transports of up to $15 \pm 10 \times 10^6\,\mathrm{m^3\,s^{-1}}$, several times the overall exchange between the Nordic Seas and the subpolar North Atlantic. The seasonal variability of the Greenland Basin and the Norwegian Basin can be adequately modelled using the barotropic vorticity equation, with the wind and bottom friction as the only forcing mechanisms. For the Lofoten Basin and the Iceland Plateau less than 50% of the variance can be explained by the wind.

1. Introduction

The Nordic Seas, comprising the area between Greenland, Spitsbergen, Norway, Iceland and the Faroe Islands, are a marginal sea with great importance for the Atlantic Meridional Overturning Circulation. Atmospheric conditions in this area lead to a transformation of inflowing warm and buoyant surface water into cold and dense deep water masses (Mauritzen, 1996) that eventually feed the overflows across the Greenland–Scotland Ridge into the subpolar North Atlantic (Hansen and Østerhus, 2000). The circulation within the Nordic Seas is essential for the deep water formation as it transports the inflowing surface water northwards, redistributes the water within the Nordic Seas and supplies the overflows with the dense water to be exported.

The near-surface circulation of the Nordic Seas was studied with drogued surface drifters by Poulain et al. (1996), Orvik and Niiler (2002) and Jakobsen et al. (2003). They find a general cyclonic circulation with meridional boundary currents and additional cyclonic circulation patterns in the Greenland Basin, the Norwegian Basin and the Iceland Plateau. The surface drifters confirm the tight link between surface circulation and bottom topography that was already noted by Helland-Hansen and Nansen (1909) in their fundamental study of the Nordic Seas.

Our knowledge about the mid-depth and deep circulation of the Nordic Seas stems mainly from water mass analyses, current observations with moored instrumentation and model studies. The basin structure of the Nordic Seas (Fig. 1) with closed f/H contours and the weak stratification leads to a strong topographic steering of the flow field. This led Nøst and Isachsen (2003) to develop a simplified diagnostic model for the Nordic Seas and the Arctic Ocean that is driven by climatological wind forcing and a climatological density field. It solves for a bottom flow field which compares well with available direct current observations. The number of these direct current measurements at depth is limited for the interior of the Nordic Seas as most current meter studies concentrated on the in- and outflows to and from the Nordic Seas. An exception is the study of Woodgate et al. (1999) who deployed moorings at the continental slope east of Greenland that extended into the deeper parts of the Greenland Basin. They find evidence for a recirculation internal to the Greenland Sea that is intensified towards the edge of the basin.

Several studies show an intensification of the Nordic Seas' internal circulation in winter. This seasonal variability is found

*Corresponding author.
e-mail: gunnar.voet@zmaw.de
DOI: 10.1111/j.1600-0870.2010.00444.x

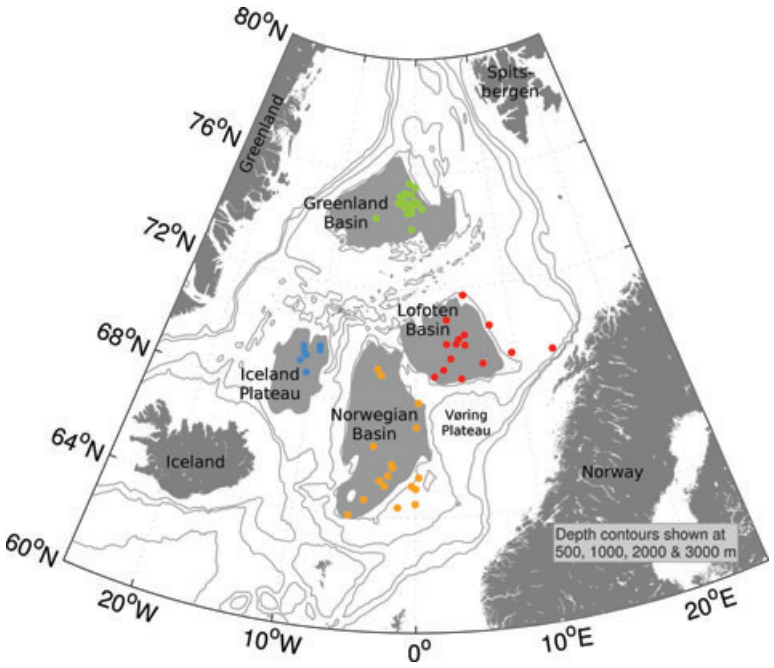

Fig. 1. Float deployment positions in the four major basins of the Nordic Seas. Deployments took place between 2001 and 2008. The area of closed bottom contours is shown in grey for each basin. The encircling depth contours are about 1600 m for the Iceland Plateau and about 3000 m for the Greenland, Lofoten and Norwegian Basins.

in the surface circulation (Jakobsen et al., 2003), in current meter records at the Greenland shelf break (Woodgate et al., 1999), in the steric height of the water column (Mork and Skagseth, 2005) and in a diagnostic model by Isachsen et al. (2003). Contrary to these indications for a strong seasonal variability of the Nordic Seas circulation, the dense overflows across the Greenland–Scotland Ridge are remarkably stable on time scales longer than a few weeks. No seasonal variability was found in the overflow through Denmark Strait and it is only intermittent in the Faroe Bank Channel (Quadfasel and Käse, 2007).

Since 2001 current measurements have been made in the Nordic Seas by use of profiling Argo floats. The floats drift at depths of 1000 and 1500 m and this allows one to study the mid-depth flow below the upper Atlantic and Polar layers in detail. The main questions we want to answer are (1) What is the mean pattern of the circulation at mid-depth? (2) Is there a seasonal cycle in the strength of the deep circulation—similar to that in the surface layer—that contrasts the stability of the dense overflows? and (3) What are the driving mechanisms for the mid-depth circulation of the Nordic Seas?

The paper is structured as follows. Section 2 gives an overview over the data used in this study, the method for calculating the deep drift of the floats and an error estimate thereof. In Section 3, we analyse the topographic steering of the flow field before we calculate the time-mean circulation scheme at depth in Section 4. The seasonal variability of the gyres in the basins and forcing mechanisms are analysed in Section 5. Conclusions are drawn in Section 6.

2. Data and methods

2.1. Float data set

Within the Argo project a total of 61 profiling floats have been deployed in the Nordic Seas through February 2009. The aim of Argo is to establish a global array of profiling floats in the world oceans providing hydrographic data to estimate the large-scale geostrophic flow field (Roemmich et al., 1999). Profiling floats are autonomous drifters equipped with sensors to record vertical profiles of temperature, conductivity and pressure and in certain cases even more parameters like oxygen and fluorescence (Gould, 2005). Floats are passive drifters in the horizontal, but they can adjust their buoyancy to control their vertical movements. Most of the time the floats stay at a parking depth that is set prior to their deployment. The floats deployed in the Nordic Seas were programmed for a parking depth of 1000 m except for seven floats in the Norwegian and Lofoten Basin that were set to a parking depth of 1500 m. After drifting at their parking depth for around 9 d, the floats descend to 2000 m, ascend to the surface while recording a profile of the water column, stay at the surface for 5 h to transfer their data and position to a satellite until they descend back to the parking depth. This whole cycle takes 10 d and is repeated by the floats until eventually the lifetime of their batteries is reached.

Profiling floats were deployed in all basins of the Nordic Seas (Fig. 1). The deployments started in summer 2001 and more than 4100 profiles were obtained by these floats through the last data update for this study in February 2009. The positions of

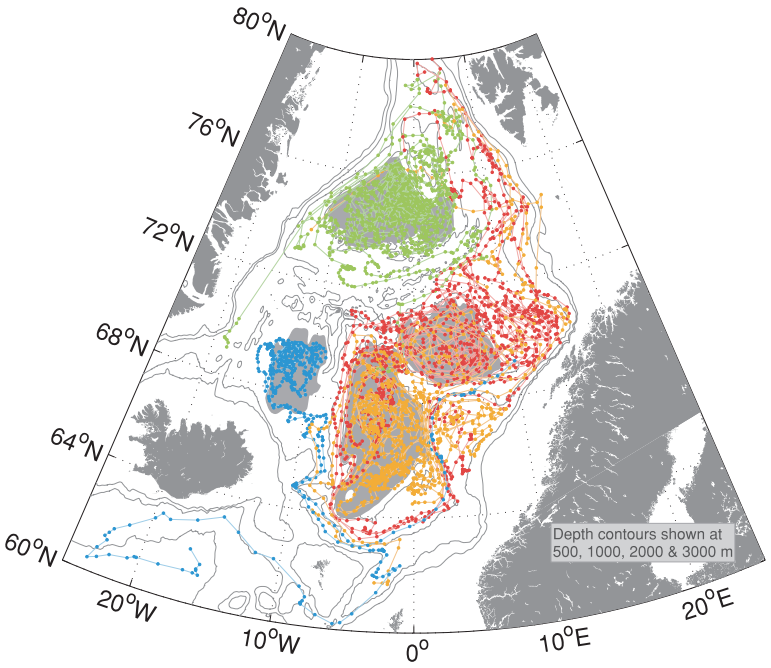

Fig. 2. Positions of all profiles recorded by the floats in the Nordic Seas. The colours of the profile positions correspond to the basin they were deployed in (see Fig. 1).

all profiles recorded by the floats are shown in Fig. 2. With the growing number of floats in the Nordic Seas the data density increased from around 15 profiles per month in the early years to around 70 profiles per month at present (Fig. 3).

We use the surface position data of the floats to estimate the flow field at mid-depth. In principle, these measurements are not truly Lagrangian, due to the surfacing of the floats every 10 d and the inability of the floats to follow vertical motion, but the drift of a float during one cycle is still a sound measurement of the water mass pathway integrated over 10 d. This is shown in a comparison between drifts measured by acoustically tracked RAFOS floats and profiling floats by Machín et al. (2006). Their study shows no significant difference between the results from the two instrument types, the only drawback of the profiling floats being that eddy variability at short time scales is not resolved. The surfacing of the floats even has an advantage. It improves statistics compared to the RAFOS floats as it leads to a decorrelation of the single displacements at depth and thereby increases the number of degrees of freedom (Davis, 1998).

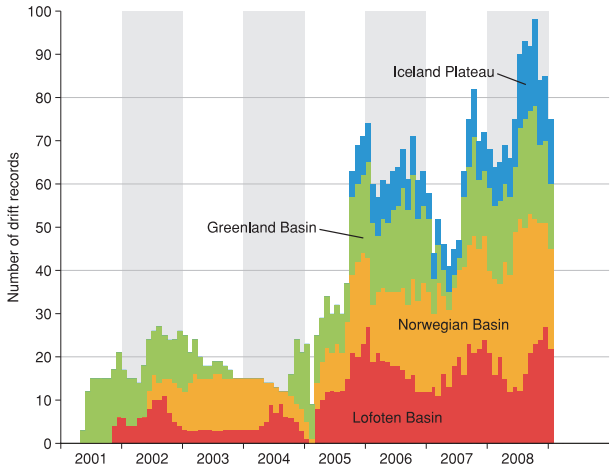

Fig. 3. Number of profiles per month recorded by the floats for each basin of the Nordic Seas.

All observations deriving from the two different float parking depths were treated as mid-depth and no recalculation of the 1500 m data has been done to lift them up to 1000 m. Below the relatively warm and saline Atlantic and the cold and fresh Arctic water masses at the surface, the stratification in the Nordic Seas is weak. The largest depth reached by the Atlantic water masses is found in the Lofoten Basin with approximately 800–900 m (Orvik, 2004). Thus, below 900 m geostrophic shear should be weak. Calculations with the float profile data from the Nordic Seas confirm that between 1000 and 1500 m the velocity difference is less than 0.3 cm s^{-1} except for a small area in the Lofoten Basin where it can be up to 0.7 cm s^{-1}. We therefore treat both parking depths as one level.

In certain cases of shallow bathymetry the floats may hit the bottom and get stuck when attempting to descend to the profiling depth of 2000 m. This happened only after the drift at the parking depth and in all cases the sensors showed no sign of a delayed ascent to the surface thereafter, indicating that no trapping of floats at the seafloor occurred.

2.2. *Estimating the deep drift from surface positions*

To calculate the drift of a float at depth, we take the last surface position before its descent to the parking depth, the first

surface position after the ascent back to the surface and the time interval between these two positions. The drift velocity then is the distance between the two positions divided by the time interval. We define the location and time of the velocity observation as the mid-point between the diving and surfacing points. Two main error sources have to be considered when the surface positions of the floats are used to infer the drift at depth. These are the uncertainty of the position fix and the velocity shear the float encounters on its passage between surface and depth.

The uncertainty of the position fix is influenced by two factors, the technically limited accuracy of the satellite positioning system and the non-continuous measurement of the surface position. The accuracy of the CLS-Argos positioning system is always better than 1500 m with a mean uncertainty of 800 m for all position data used in this study. This corresponds to a velocity error of less than 0.2 cm s^{-1}. The mean distance that a float covers within one subsurface cycle is 35 km, the median is 28.5 km (Fig. 4). Thus, the error arising from positioning inaccuracy is less than 5% for most of the measurements, except for very low drift velocities and hence short drift distances. The measurement interval of the surface position depends on the frequency of satellite overpasses. A long time interval between the position measurements can lead to a considerable time lag between the real surfacing position of the float and the first position fix by the satellite. The same holds for the diving position. Park et al. (2005) developed a routine that extrapolates the surfacing and diving positions from the positions fixed by the satellite and thereby increases the accuracy of the deep drift estimate. We do not use this method for two reasons. First, the large satellite coverage at the high latitudes of the Nordic Seas reduces the mean time interval between single position fixes to only 14 min. This results in an uncertainty of the real diving and surfacing position that is smaller than the spatial uncertainty of the position fix itself. Second, the method of Park et al. (2005) requires the exact surface arrival time that usually is part of the metadata. Unfortunately, this data set is incomplete for our Nordic Seas floats. We therefore simply use the first and last position fix, treating them as the real surfacing and diving points.

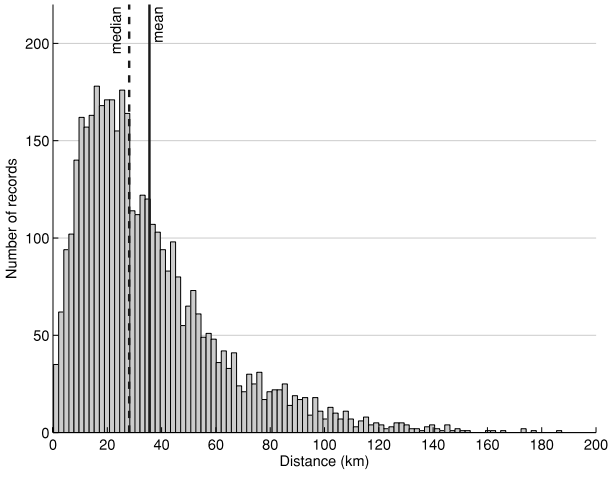

Fig. 4. Histogram of the distances covered by the floats during individual cycles. The straight line shows the mean of the distribution, the dashed line gives the median.

A simple approach for estimating the influence of the velocity shear between surface and depth on the calculation of the drift velocity at depth is a linear interpolation between surface and deep velocity (Lebedev et al., 2007). The mean surface velocity during the time interval the float stays at the surface, calculated by a least squares fit to the surface positions, is 20 cm s^{-1}. The mean velocity at depth, calculated from all float displacements, is about 4 cm s^{-1}. Thus, during the 2 × 7 h of ascent and descent between surface and parking depth the mean velocity is 12 cm s^{-1}. With the mean vertical velocity of a float of 0.08 dbar s^{-1} this results in a maximum displacement of about 5 km during the round-trip between depth and surface. This is the upper limit for the error deriving from velocity shear which may not be reached in all cases.

Surface velocities are dominated by Ekman drift and inertial currents that influence only the upper part of the water column. As the float is at the surface for only five hours the contribution of inertial currents to the surface flow is random in its direction. An analysis of the wind direction over the Nordic Seas shows that it is randomly distributed over the Norwegian and Lofoten Basins while over the Greenland Basin and the Iceland Plateau winds from the north are dominating. Consequently, the Ekman drift is also randomly directed in the Norwegian and Lofoten Basins while it is expected to have a preferred direction in the Greenland Basin and Iceland Plateau. When averaging over a number of records, the influence of inertial currents and, at least for the Norwegian and Lofoten Basins, the Ekman drift is expected to cancel out.

We tested the influence of the surface velocity on the deep velocity estimate by omitting the surfacing completely, i.e. by only taking one random surface position per surfacing. With the deep drifts calculated from these positions only, the results reported in this paper are only slightly altered. This supports the assumption of the surface velocities being, at least to some extent, random noise that averages out when calculating mean values from a larger number of observations.

There is another factor that may systematically decrease our velocity estimate. We assume the deep drift to be a straight line between the two surface position fixes. The topographic steering of the flow in the Nordic Seas (see below) should lead to a more complex path of the flow that can only be of equal length or longer than a straight line. We cannot account for this underestimate in our velocity calculation as we are lacking any position information between the surface position fixes. When comparing the float measurements with Eulerian measurements from moorings this effect has to be kept in mind.

2.3. Wind stress data

To estimate the atmospheric wind forcing over the Nordic Seas, NCEP/NCAR-reanalysis data (Kalnay et al., 1996) are used. The NCEP/NCAR-reanalysis assimilates a multitude of observations into a model to produce a homogeneous data set of many atmospheric and oceanic variables. A comparison with QuikSCAT wind fields, a data set derived from active radar measurements of the sea surface roughness, has shown that the NCEP/NCAR-reanalysis data represents the surface winds over the Nordic Seas well in terms of low- and high-frequency variability (Kolstad, 2008). We use the 6-hourly momentum flux data set to calculate the wind stress curl over the Nordic Seas.

2.4. Bottom topography

The ETOPO2 bathymetry with a resolution of two minutes is used to assign bottom depths and topographic gradients to the float displacements. For the region of the Nordic Seas, ETOPO2 consists of the Smith and Sandwell bathymetry (Smith and Sandwell, 1997) south of 64°N and the International Bathymetric Chart of the Arctic Ocean (IBCAO, Jakobsson et al., 2000) north of 64°N. For the calculation of bottom gradients we smoothed the topography at the length scale of the float displacements (Thomson and Freeland, 2003). The mean displacement for all Nordic Seas floats is about 30 km and we remove scales smaller than 40 km.

3. Topographically influenced mean flow

The floats have the tendency to stay in the basin where they were deployed in (Fig. 2). On average 75% of all float positions stem from the deployment basin while the remaining 25% are located in one of the other basins. There is some organized exchange through the opening between the Norwegian and Lofoten Basin with floats leaving the Norwegian Basin with the rim current in the southern part of the opening. Floats only transfer from the Lofoten into the Norwegian Basin in the northern part of the opening. Furthermore, some floats leave the Lofoten Basin in the rim current towards Fram Strait, one float leaves the Greenland Basin southward in the rim current. The floats' stay in the Iceland Plateau is rather short, and most of them escape towards the southeast into the Norwegian Basin within one to 2 yr. One float from the Iceland Plateau even made its way through the Faroe Bank Channel into the subpolar North Atlantic. However, the Iceland Plateau is an exception and the floats mostly stay in the basin they were deployed in.

In general the floats follow lines of constant bottom depth. Examples for single trajectories can be found in Gascard and Mork (2008) and Søiland et al. (2008). In Fig. 2 the positions of two floats above the only 1000–1500 m deep Vøring-Plateau off the Norwegian coast between the Lofoten and Norwegian Basin show that they were trapped there. This indicates again the topographic steering of the flow field as the floats and thus the water cannot move away from the relatively shallow plateau into deeper areas.

Given the strong topographic steering we project the measured drift velocities onto the bathymetry. This gives us velocity components along and across the local topography instead of north and east components. The convention here is that for the along bathymetry component, positive values have the shallow bottom on the left side irrespective of the basin.

Figure 5 shows the distributions of the along and across bathymetry velocity components of all drift records, both for regions of strong and weak topographic gradients. They differ in two aspects. First, the distribution of the along component is broader compared to that of the across component. Thus the variation of the along topography flow is larger than that of the across component. Mesoscale variability is expected to be isotropic and the variance of the currents in both along and across bathymetry direction should be equal. The larger along topography variance indicates that another process is acting on this component. Below we will show, that the increase of variance is due to the seasonal cycle of the flow. Second, while the across component is distributed around zero, the along component is shifted towards negative velocities, most pronounced in the rim currents. This negative shift of the along bathymetry component corresponds to a mean cyclonic circulation. The corresponding distributions for the individual basins show the same structure in each of the four basins.

The dependence of the along bathymetry velocity component on the size of the bottom slope is shown in Fig. 6. While single data points exhibit a large variability, the bin-averaged values show an increase of the velocity with steeper bottom slope. The

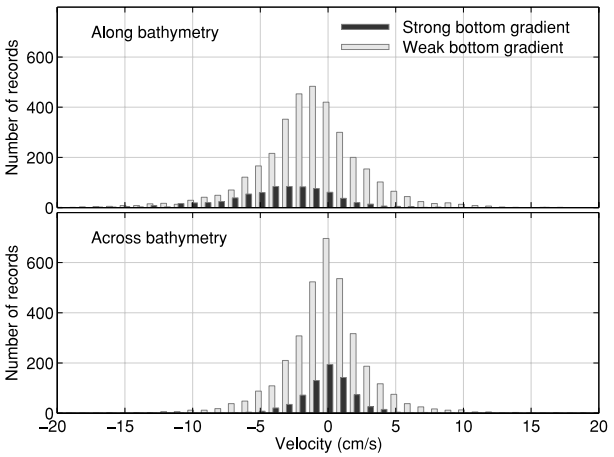

Fig. 5. Histogram of the velocity components along bathymetry (upper panel) and across bathymetry (lower panel) with distinction between velocities over strong (>0.015) and weak bottom gradient (≤0.015). The mean values for both distributions of the across component are not significantly different from zero while for the along component the mean values are -3.5 cm s^{-1} over strong and -1.3 over weak bottom gradient.

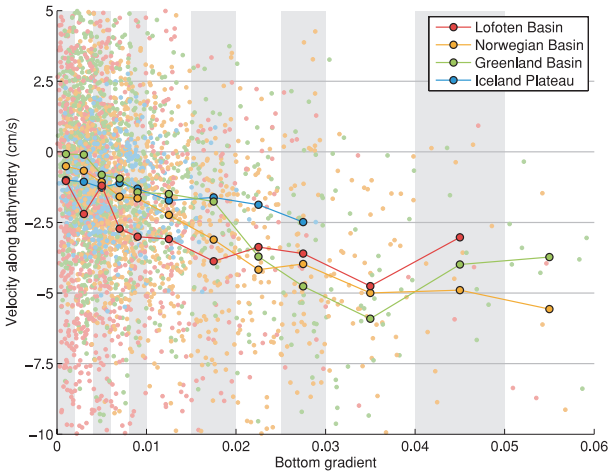

Fig. 6. Dependency of the along bathymetry velocity component on the bottom gradient for the four basins. Individual observations are marked with small dots. Not all individual data points are shown in this figure. The individual observations averaged into bottom gradient bins are shown with bold markers. For weak bottom gradients, where many observations are available for averaging, the width of the bins is smaller than for strong bottom gradient, where the data is sparse.

velocity is negative which stands again for cyclonic flow. The intensification of the flow with increasing bottom gradient is evident in all four basins of the Nordic Seas. The average over all basins shows a linear increase of the velocity with the bottom gradient until a maximum value is reached at a gradient of about 0.03. From thereon, the mean velocity is approximately constant.

The dependence of the current velocity at depth on the size of the local bottom gradient confirms the results of Nøst and Isachsen (2003). They show that within closed f/H contours the bottom velocity is dependent on the local slope of the f/H field and on the integrated forcing within that contour. We will come back to the latter point when analysing the forcing of the seasonal variability of the circulation.

4. Time-mean mid-depth circulation

4.1. Mean circulation scheme

For the construction of a mean circulation map at the float parking depth the data set is averaged over the whole period 2001–2009. The map is calculated by assigning each float observation to the nearest point of a rectangular grid with the size of one degree latitude, i.e. about 110 km. The calculation of the distance between observation and grid point takes the topographic steering of the flow into account. It thus models the longer correlation scales along bottom topography. Following Davis (1998), the effective distance r between float observation and grid point is calculated as

$$r^2 = |\mathbf{x}_a - \mathbf{x}_b|^2 + \left| 3\lambda \frac{H_a - H_b}{H_a + H_b} \right|^2, \qquad (1)$$

where the first term on the right-hand side gives the geographical distance between observation and grid point. Here $\mathbf{x}_a$ denotes the position of the grid point and $\mathbf{x}_b$ the position of the mid-depth observation. The second term with the bottom depths H_a and H_b at the points $\mathbf{x}_a$ and $\mathbf{x}_b$ increases the effective distance according to the difference in bottom depth between observation and grid point. The topography parameter λ was chosen to be 100 km as in Lavender et al. (2005). The bottom depths for the calculations were obtained from the smoothed ETOPO2 bathymetry data set. After assigning each observation to its nearest grid point, the mean velocity and direction at each grid point are calculated as the mean over all observations the grid point comprises.

The resulting pattern of the mid-depth circulation is shown in Fig. 7. Velocity vectors are only shown at grid points where at least five data points are available. Figure 8 gives the number of observations that were used in the calculation of the mean velocity vectors. Cyclonic gyres are found in each of the basins. They are intensified towards the rims. In the centre of the basins the velocities are relatively small and more randomly directed. The largest variability (not shown) is found at the rim while it is low in the centre of the basins. An exception is the Lofoten Basin where the variability in the centre is almost as high as at the rims. As already indicated in Fig. 2, we do not find a strong mean advection between the basins of the Nordic Seas. Exceptions are the export of floats from the Iceland Sea to the Norwegian Basin and some exchange between Lofoten and Norwegian Basin due to gaps in the topographic barrier between these two basins. The small exchange of floats between the basins does not mean that there is no exchange of water masses between the basins though. Transports can happen in narrow, jet-like currents that floats are not capable of covering adequately.

The circulation at mid-depth generally has the same pattern as the surface circulation shown in the study by Jakobsen et al. (2003). They also find cyclonic recirculation in the Greenland Basin, the Iceland Plateau and the Norwegian Basin. Their surface flow pattern in the Lofoten Basin is directed northwards at the eastern and western edge of the basin and thus has both a cyclonic and anticyclonic component. This is in contrast to our finding of a strong cyclonic gyre at mid-depth and implies a considerable shear between surface and mid-depth flow in the western part of the Lofoten Basin. The mid-depth circulation found here is also very similar to the model results of Nøst and Isachsen (2003) who show a scheme of the bottom-near circulation in the Nordic Seas. This confirms their simple and elegant model and also agrees with the few mooring current measurements they used to validate their model output. The small and randomly directed velocities in the centre of the gyres agree with the mooring records from the Greenland Basin of Woodgate et al. (1999).

For an estimate of the statistical robustness of the mean circulation scheme we calculate the statistical uncertainty of the mean velocities following Lavender et al. (2005) as the covariance of each average divided by the number of degrees of freedom in

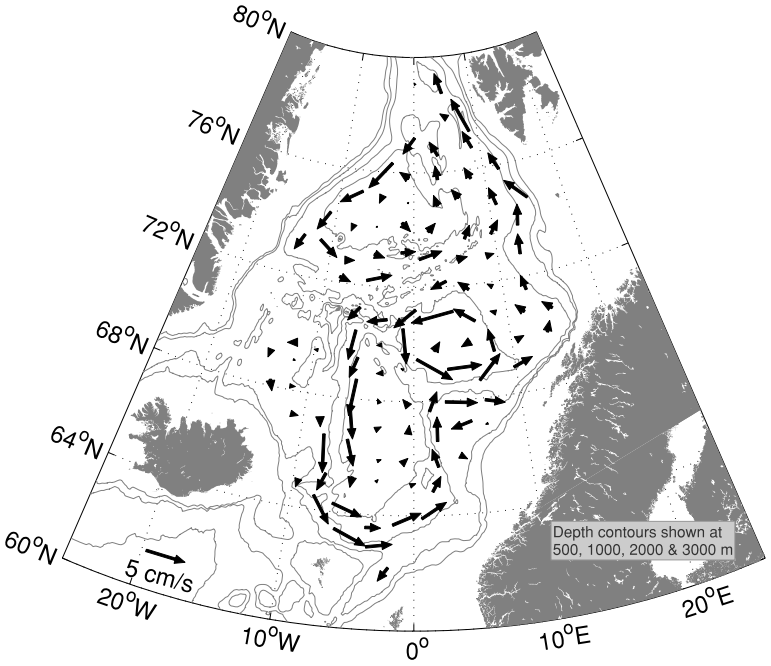

Fig. 7. Time-mean mid-depth circulation of the Nordic Seas on a rectangular grid with a size of 110 km. Only mean values calculated from more than five observations are shown.

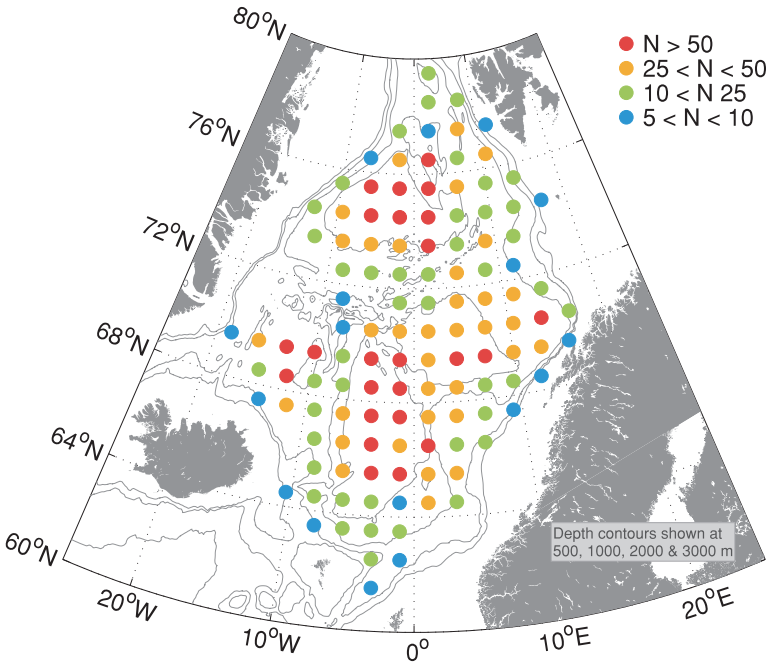

Fig. 8. Number of observations per grid cell used for the calculation of the mean velocities.

the average. Each observation contributes a degree of freedom unless it is correlated with another observation in the same grid cell. For different floats there is no correlation as the floats did not encounter each other close enough in time and space. For a single float, successive observations may very well be correlated with each other. However, the time lagged autocorrelation for single floats in our data set shows that the observations are decorrelated after about 10 d, indicating that consecutive subsurface drifts are essentially uncorrelated. A conservative estimate of the Lagrangian integral time scale is to take the decline in the autocorrelation in both directions. This results in a time scale of about 20 d. Dividing the time a single float spends in a grid cell by this decorrelation time scale gives the degrees of freedom it contributes. A decorrelation time scale of 20 d is consistent with the results of Lavender et al. (2005) who also use this value for the double-sided decorrelation time scale. The statistical

uncertainties calculated with this integral time scale show that most mean velocities are significant. Only few mean velocities in the centre of the basins are smaller than their statistical uncertainty.

4.2. Topostrophy

It is instructive to study the topographical steering of the flow with a single scalar parameter. Killworth (1992) introduced such a parameter to measure the alignment of the flow with bottom topography. Holloway et al. (2007) termed this parameter topostrophy. The topostrophy T is defined as the vertical component of the cross product of velocity vector and bottom gradient:

$$T = (\vec{v} \times \vec{\nabla} H)_z, \tag{2}$$

Topostrophy is positive for cyclonic flow and negative for anticyclonic flow. It is zero for a current perpendicular to local isobaths. We define the normalised topostrophy $\hat{T}$ as

$$\hat{T} = \frac{(\vec{v} \times \vec{\nabla} H)_z}{|\vec{v}| \cdot |\vec{\nabla} H|}. \tag{3}$$

The normalized topostrophy derived from the float velocity data set confirms the general cyclonic circulation at mid-depth in the Nordic Seas (Fig. 9). This holds particularly for the rim currents in the basins. In the interior of the basins, gradients of local topography are weak and the flow is less aligned with bottom contours. The strongest alignment with the bottom topography is found over the Iceland Plateau and in the western and southern part of the Norwegian Basin. These two areas also show relatively strong positive topostrophy away from the rim current. Slightly negative topostrophy in the centre of the Lofoten Basin and the associated anticyclonic flow confirms the findings of Köhl (2007), who detected a permanent anticyclonic 'Lofoten Vortex' in a high resolution regional model simulation.

5. Seasonal variability

5.1. Seasonal signal in the float velocity data

Previous studies of currents in the Nordic Seas revealed considerable variability on the seasonal time scale. Jakobsen et al. (2003) find an intensification of the surface flow in winter of order of 5 cm s^{-1}. Transports calculated from mooring records in the Greenland Sea (Woodgate et al., 1999) and in the Norwegian Basin (Orvik et al., 2001) are stronger in winter than in summer. Mork and Skagseth (2005) studied the seasonal variability in bottom speeds calculated from altimeter data and hydrographic data. They find a spin-up of the gyres in winter and spring in the Greenland, Norwegian and Lofoten Basin, with the highest seasonal variability in the Norwegian Basin of about 1 to 2 cm s^{-1}.

We use our float data set to estimate the strength of the seasonal cycle of the circulation at mid-depth. At the beginning of 2009, the number of observations is yet insufficient to detect the temporal variability at the spatial resolution used for our mean circulation map (Fig. 7). We therefore calculate the monthly mean gyre velocities in a geographic frame to construct velocity time series for the individual basins. The monthly mean velocity in a basin gyre is defined here as the average over all along bathymetry velocities recorded in the rim areas of the basins during one month. Figure 10 shows the data points at the rim in each basin used for the calculation. For the Greenland and Norwegian Basin, the area between the 1000 and 3000 m isobath is chosen to represent the rim of the gyres. In the Lofoten Basin we define the rim as the area between 2800 and 3200 m

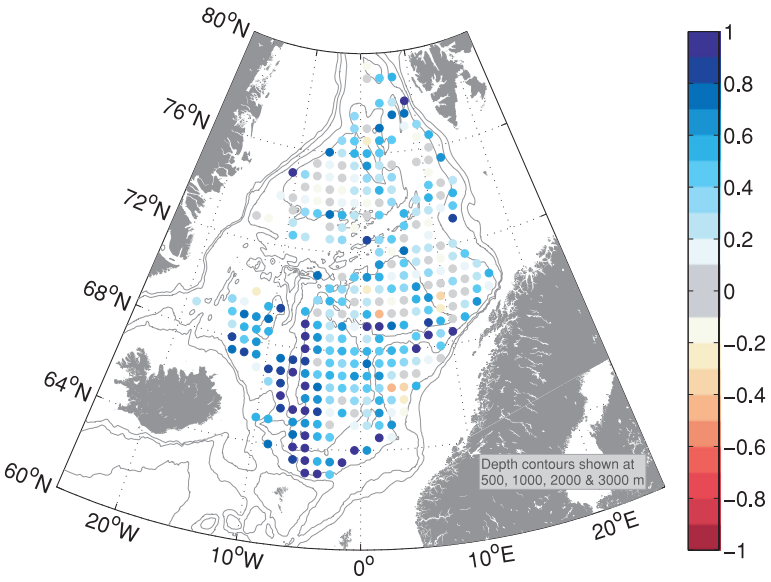

Fig. 9. Normalised topostrophy derived from the mean circulation scheme. Blue colours stand for cyclonic flow, red colours for anticyclonic flow. The closer the absolute value of the normalized topostrophy tends towards one, the more the flow is aligned to the bathymetry.

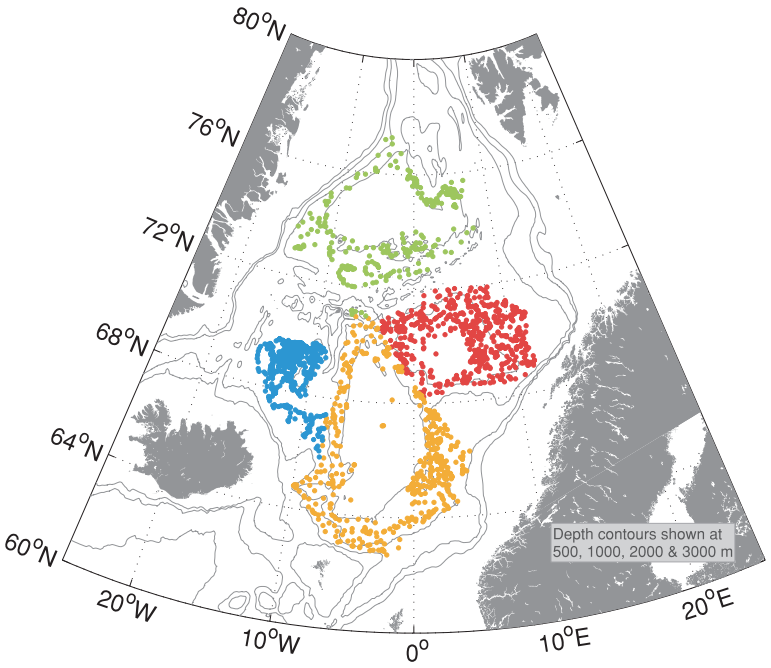

Fig. 10. Observations used to calculate mean velocities of the basin gyres. Observations between the 1000 and 3000 m isobaths were chosen to be representative for the rim in the Greenland and Norwegian Basin. In the Lofoten Basin the area between the 2800 and 3200 m depth contours defines the rim of the basin. For the Iceland Basin the whole area deeper than 1000 m is chosen.

bottom depth. This discards data at the very eastern edge of the Lofoten Basin that are not associated with the gyre circulation. For the analysis of the Iceland Plateau gyre all data are used, as it is not possible to define a rim on the relatively shallow plateau. Figure 11 shows the number of observations per month that are available for the calculation of gyre velocities in each of the basins. Using different rim definitions, as for example 2000–3000 m for the Norwegian and Greenland Basin, does not change the results in a qualitative way but only results in a small change in the amplitude of the seasonal cycle.

The rationale for using only rim data is twofold. First, velocities in the centre of the gyres are small and often not aligned with topography. This can be seen in the mean mid-depth circulation scheme (Fig. 7). Second, when analysing the forcing of the seasonal variability below, we will use a barotropic vorticity equation to describe the temporal evolution of the basin gyre velocities. In this equation, the velocities at the rim of the gyres are used.

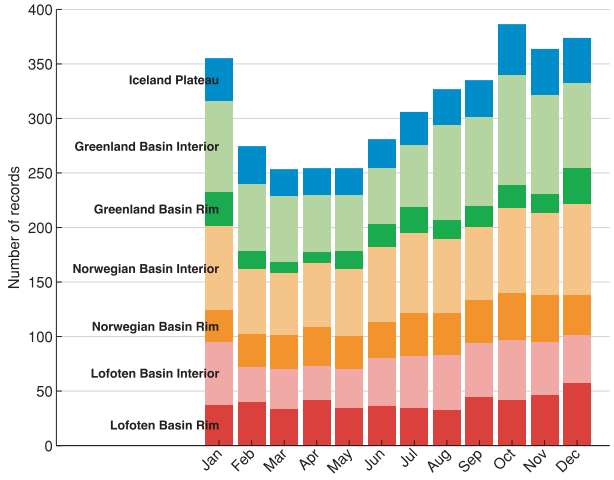

Fig. 11. Number of records used for the calculation of the monthly mean basin gyre velocities.

The method of calculating monthly mean gyre velocities from the float observations is problematic due to the position and time of the deployment of the floats. Most floats were deployed in the centres of the basins (Fig. 1) during cruises that took place between late spring and early autumn. This uneven distribution in space and time may have an influence on the calculation of monthly mean velocities. By taking observations at the rim of the basins only, the problem of the deployment positions is minimized.

The monthly mean gyre velocities for the four basins are shown in Fig. 12. A low-pass filter (weighted three point average) is used to smooth the data for the seasonal analysis. The Greenland Basin has a seasonal cycle with higher velocities in winter and a minimum velocity in late summer as has the Norwegian Basin. The peak-to-peak amplitude of the seasonal variability is about 3 cm s^{-1} for the Greenland Sea and 1.5 cm s^{-1} for the Norwegian Basin. In the Norwegian Basin, a semi-annual cycle seems to be superimposed on the seasonal cycle. The observations over the Iceland Plateau also show lower velocities in summer than in winter, but the amplitude is small with only about 0.5 cm s^{-1}. This low amplitude matches with the low mean velocities found over the Iceland Plateau (Figs 6 and 7).

In the Lofoten Basin we do not find a clear seasonal cycle as in the other basins. Here low velocities occur in winter and maxima are seen in early summer and early winter. Peak-to-peak changes

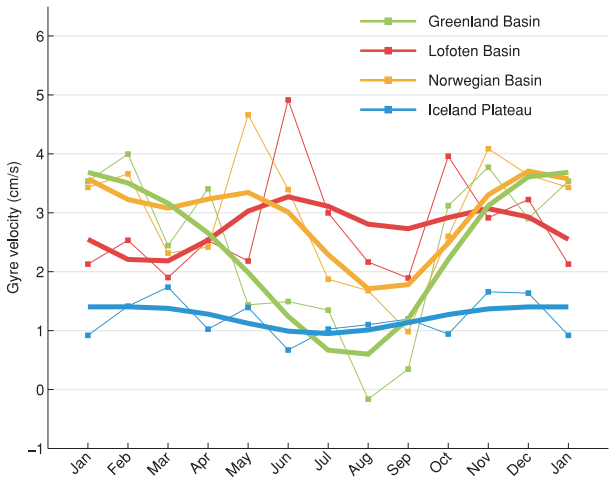

Fig. 12. Seasonal variability of the gyre velocity in the four basins. The gyre strength is defined as the mean velocity along the bathymetry at the rim of the gyre. Thin lines with markers give monthly mean values, thick lines show a low-pass filtered version (weighted three-point average) of the monthly values. The standard deviation for the monthly mean values (not shown in the figure) is about 4–6 cm s^{-1} for all months and basins. This statistical uncertainty reflects the mesoscale variability that is not resolved by the measurement cycle of the floats of around ten days.

are just over 1 cm s^{-1}. This is quite in contrast to the pattern in the other basins which may have several reasons: On the one hand, it is not clear whether this result is still influenced by the many observations from the eastern part of the basin (Fig. 10). The scheme of the time-mean circulation (Fig. 7) shows that the flow diverges in this area. In addition, the eastern part of the Lofoten Basin is an area of high eddy kinetic energy (Gascard and Mork, 2008) that could influence the calculation of the mean gyre velocity. On the other hand, the layer of warm Atlantic water spreads over the whole surface area of the Lofoten Basin and deepens considerably. This could lead to forcing mechanisms different from the other basins resulting in a different seasonal cycle. We come back to this when analysing the forcing of the seasonal variability by the wind stress below.

5.2. *Wind forcing*

The mean wind forcing over the whole Nordic Seas is cyclonic and has a pronounced seasonal cycle (Jónsson, 1991). Figure 13 shows the monthly mean wind stress curl for each basin of the Nordic Seas calculated for the period when floats were present in the basin. These periods are also representative for the complete 60 yr NCEP record except for the Iceland Plateau where the wind stress curl in March and November is considerably smaller in the float period. Overall the mean wind stress curl has a clear seasonal cycle. The maximum of the curl occurs in winter while it is almost zero in the summer months. The strength of the seasonal momentum forcing is largest in the Greenland Basin and smallest over the Norwegian Basin. Our float observations fall into a period with a moderately high (0.5) NAO Index. The state of the NAO is very important for the wintertime wind speeds in the Nordic Seas, with a high correlation between positive NAO Index and wintertime wind speeds (Kolstad, 2008). Numeric simulation results of Serra et al. (2010) also show the correspondence between decreasing NAO Index and less cylonicity of the Nordic Seas gyre circulation.

5.3. *Forcing of the circulation*

The ocean has a barotropic and a baroclinic response to the wind forcing by radiating barotropic and baroclinic planetary waves. The time scale for the adjustment of a basin of the size of the Nordic Seas at high latitudes is several years for the baroclinic waves but only some days for the barotropic waves. Thus, the seasonal variability of the wind forcing cannot be compensated by baroclinic oceanic processes and only a barotropic response of the ocean to the wind forcing can be expected.

From weather maps, Aagaard (1970) calculated monthly mean Sverdrup transports for the Nordic Seas and found transports exceeding 30 Sv (1 Sv = 10^6 m^3 s^{-1}) at the western boundary of the Nordic Seas. He assigns this strong transport to the internal gyre recirculation. The variability between different months is large in his calculations. However, the order of 30 Sv, also estimated by Jónsson (1991) from wind observations, agree with estimates from current measurements (Aagaard, 1970; Woodgate et al., 1999), suggesting that the wind field is able to maintain the internal gyre circulation, at least at the western boundary in the Greenland Sea. Mork and Skagseth (2005) study the relation of the wind forcing over the Norwegian Basin to the observed seasonal cycle of the bottom flow speed. Using a harmonic fit to both cycles, they show that the phase of the wind forcing is able to explain the observed changes in the flow speed.

To analyse the influence of the wind forcing on the seasonal variability of the flow field derived from the float data (Fig. 12) we use a vertically integrated stream function describing the vorticity input to the Nordic Seas. The use of a vertically integrated stream function is justified as the stratification in the Nordic Seas is weak. With the stream function Ψ of the vertically integrated volume transport and a rigid lid approximation, Marotzke and Willebrand (1996) obtain the equation for the barotropic vorticity

$$\frac{\partial}{\partial t}\left(\vec{\nabla}\cdot\frac{1}{H}\vec{\nabla}\Psi\right)+\vec{\nabla}\Psi\times\vec{\nabla}\frac{f}{H} = \vec{\nabla}\times\frac{\vec{\tau}_w-\vec{\tau}_b}{H}+\vec{\nabla}E\times\vec{\nabla}\frac{1}{H}+\ldots \quad (4)$$

with wind stress $\vec{\tau}_w$ divided by surface density, bottom stress $\vec{\tau}_b$, bottom depth H and the potential energy E of the stratification. The second term on the right is the bottom torque that expresses

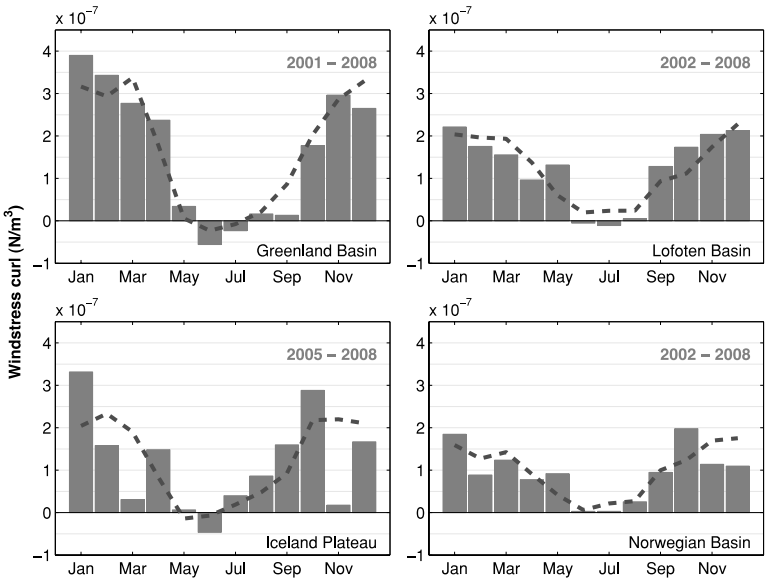

Fig. 13. Monthly mean wind stress curl integrated over the basins of the Nordic Seas (bars). The wind stress curl is calculated from NCEP/NCAR reanalysis momentum fluxes. The time periods used to calculate the mean values correspond to the time that floats stayed within the basin. The dashed lines show the seasonal cycle of the wind stress curl for the whole 60 years of the NCEP/NCAR reanalysis period 1948–2008. The area of the basins is defined by the 1200 m depth contour for the Iceland Plateau, by the 1000 m isobaths for the Greenland and Norwegian Basins and by the 2800 m depth contour for the Lofoten Basin.

the effect of potential energy gradients along lines of constant bottom depth. Non-linear terms are neglected here. The steady state solution of this equation for a basin with constant bottom depth is the well-known Sverdrup relation.

The integration around closed f/H contours simplifies the barotropic vorticity equation. The bottom torque term involves the Jacobian with $1/H$ and vanishes identically when integrated around a closed f/H contour. Isachsen et al. (2003) show in their model of the Nordic Seas that the bottom torque term is in fact small compared to the other terms. Using Stokes' theorem, the barotropic vorticity equation can be reduced to

$$\frac{\partial}{\partial t}\oint_C \vec{v}\mathrm{d}\vec{r} = \int_A \frac{\vec{\nabla}\times(\vec{\tau_w}-\vec{\tau_b})}{H\rho_0}\mathrm{d}A. \tag{5}$$

This relates the temporal change of the barotropic velocity integrated around a closed contour C to the curl of wind and bottom stress integrated over the area A confined by C.

All terms of the simplified barotropic vorticity equation can be calculated using the float measurements of the seasonal cycle of the basin gyre velocities and the reanalysis data for the wind forcing. The bottom drag is calculated from the gyre velocities observed by the floats applying a linear drag law

$$\vec{\tau}_b = R\cdot\vec{v}. \tag{6}$$

Here we assume that the observed mid-depth velocities are also representing the near bottom velocities. The unknown drag parameter R is finally derived by optimising the sum of wind and bottom drag to the observed velocity change. This gives drag parameters for each basin in the range between 5×10^{-4} and $10\times10^{-4}\,\mathrm{m\,s^{-1}}$ which is of the same order of magnitude used in the model of Isachsen et al. (2003).

As f varies only little at these high latitudes, depth contours are used instead of f/H contours for the integrals around C and over A. To be consistent with the velocity calculations we use the same basin definitions as above—1000 m for the Greenland and Norwegian Basins, 2800 m for the Lofoten Basin and 1200 m for the Iceland Plateau.

When the variability in the system is driven by the wind and bottom friction only, the sum of these two should match the observed changes of the gyres on the seasonal time scale. Figure 14 compares the observed change of the gyre velocities (left-hand side of eq. 5) with the sum of wind forcing and bottom drag (right-hand side of eq. 5). For the Greenland and Norwegian Basins, where a seasonal cycle in the gyre velocity with a minimum in summer was observed, the wind forcing explains a large part of the observed seasonal variability. The correlation between observation and the sum of wind and bottom drag is about 0.8 in the Greenland Basin with a time lag of 2 months and also about 0.8 in the Norwegian Basin with a time lag of 1 month. This mismatch in the phasing of the signal may stem from processes not considered in our analysis. Mixed layer deepening and convection is strongest during late winter, about 3–4 months after the maximum momentum forcing. At least in the Greenland Basin this buoyancy forcing leads to an enhanced doming of the deeper water column inducing cyclonic rotation of the layer. This enhances the local baroclinic flow, acting against the weakening barotropic gyre circulation.

Processes other than the wind forcing seem to play an even more important role in the Lofoten Basin where the correlation between observed velocity change and the sum of wind and bottom drag terms is always below 0.5, no matter which time lag is applied. For the Iceland Plateau the match between observation and wind forcing is small in our analysis. The velocity change was calculated over the whole area of the Iceland Plateau and not just at the rim as should be used in eq. (5). Therefore we cannot tell whether the misfit for the Iceland Plateau is due to

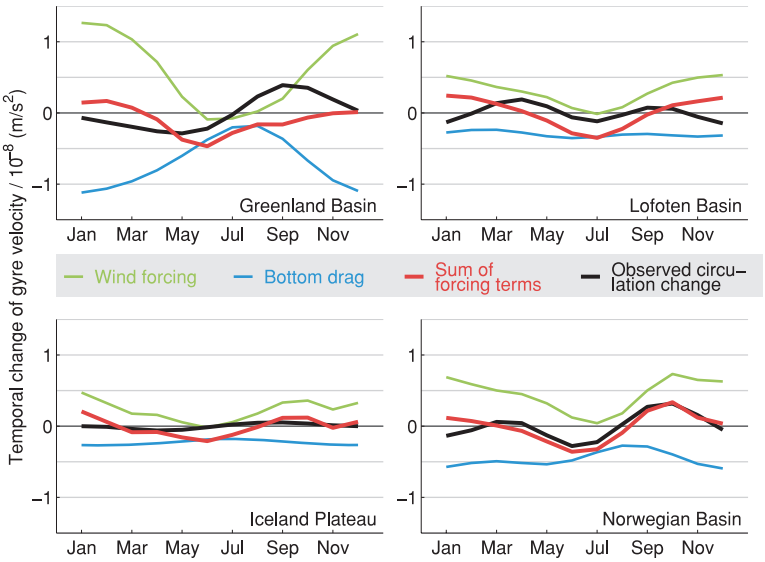

Fig. 14. Comparison of observed seasonal changes of the basin gyre circulation (black) and calculated changes from forcing terms (red). The wind forcing term is shown with the green line and the bottom friction with the blue line. The three-point weighted average version was used for all terms shown here.

the wrong velocity observation used in the analysis or associated with real oceanic processes.

The importance of the wind forcing, at least for the Norwegian and Greenland Basins, is supported by the model study of Isachsen et al. (2003) who find wind forcing more important than hydrographic (thermal wind shear) forcing for flow along f/H-contours on time scales from monthly to annual.

6. Summary and conclusions

In this paper, we have analysed the trajectories of 61 autonomous profiling floats that were deployed within the international Argo programme in the Nordic Seas between 2001 and 2009. Based on 10-d subsurface drifts between consecutive surfacing of the floats we have studied both the mean circulation at mid-depth (1000–1500 m) and its seasonal variability.

The floats were initially deployed near the centres of the four basins—the Greenland, Lofoten and Norwegian Basins and the Iceland Plateau (Fig. 1). It turned out that float diffusion between the basins was small and most floats stayed within their home topographic structure throughout their lifetime (2–5 yr). There were regional differences, though. The Greenland Basin appears to be very isolated while the two eastern basins, being swept by the northward flowing Atlantic water, suffered a larger loss of floats to their neighbours. In all, however, only 25% of the floats escaped and moved to another basin or region. This certainly indicates that the overall mean advection in the Nordic Seas is limited to the narrow boundary currents and the exchanges between the gyres and the boundary flow are dominated by diffusive processes, such as mesoscale or submesoscale processes rather than advection.

The forcing for the Nordic Seas circulation consists of three mechanisms that are drivers for a cyclonic circulation: momentum forcing, heat fluxes and freshwater input. The Nordic Seas are exposed to strong momentum forcing, with the Greenland High and the Icelandic Low being the permanent features of the atmospheric pressure pattern. Both, buoyancy and momentum forcing, drive the cyclonic circulation internal to the Nordic Seas that may be viewed as a northern extension of the North Atlantic's Subpolar Gyre, albeit with regional characteristics due to the limited exchange across the Greenland–Scotland Ridge. Momentum and buoyancy forcing are both characterized by large seasonal variability. Winter heat fluxes to the atmosphere may reach 300–400 W m^{-2} whereas during summer the ocean is gaining heat at a rate of up to 150 W m^{-2}. River run-off is largest in spring, after snow melt. Likewise, the momentum fluxes, expressed as the curl of the wind stress, range between 0 and 4×10^{-7} N m^{-3} in summer and winter, respectively.

The mid-depth flow in all basins is cyclonic, which is consistent with the surface flow (Jakobsen et al., 2003). This does not really come as a surprise, given the three cyclonic forcing mechanisms. Near the rim of the basin gyres mean current speeds are 1–3 cm s^{-1} whereas in the centres they are reduced to less than 1 cm s^{-1}. Overall the flow pattern documents the tight topographic control of the circulation as a result of the weak stratification. The velocities (see Fig. 6) translate into mean internal gyre transports of up to 15 Sv, several times the overall exchange between the Nordic Seas and the subpolar North Atlantic.

The seasonal variability of the gyre circulation within the Greenland and Norwegian Basins is large and in magnitude comparable to that of the mean flow. The tight phase link to the momentum forcing suggests that the seasonal circulation is a barotropic response to the winds and that baroclinic effects like convection only play a minor role for setting up the currents on the basin scale. When balancing the vorticity input by the winds with the losses due to linear bottom friction we estimate drag coefficients between 5 and 10×10^{-4} m s^{-1},

reasonable values that fall into the same range as those used in numerical model simulations. Estimated transport variability is up to 15 ± 10 Sv, a value confirmed by earlier direct current measurements using moored instrumentation (Woodgate et al., 1999). Over the Iceland Plateau the seasonal wind forcing is less pronounced compared to the Greenland Sea. Here the gyre circulation shows the smallest seasonal variations, consistent with the forcing. Also, the topographic gradients are much weaker than in the other basins and the flow may not be subject to as rigorous a topographic control as in the other regions. In addition, our database here is smallest and it may not be sufficient to detect the variability.

The largest deviation from our simple barotropic response model occurs in the Lofoten Basin. The gyre circulation here contains a strong semi-annual component comparable in magnitude to the seasonal signal. The reason for this is not clear to us. The forcing, wind and bottom friction, is clearly seasonal, but the float exchange with the Norwegian Basin in the South and the continental slope region in the West Spitsbergen Current in the North suggest a weaker topographic control of the flow. Results from a numerical model simulation confirm this behaviour (Serra et al., 2010). The Lofoten Basin is a region of enhanced mesoscale variability generated by baroclinic instabilities of the flow, first described by Helland-Hansen and Nansen (1909) as puzzling waves and also observed in drifter studies (Poulain et al., 1996; Jakobsen et al., 2003; Rossby et al., 2009). These baroclinic effects may also play a role in setting up the circulation, but our data set does not allow to explore such mechanisms.

The Nordic Seas are a region of intense water mass transformation. Here, through heat loss, freshwater input and melting and freezing of sea ice, buoyant Atlantic Water is transformed into buoyant (cold, low salinity) near surface waters and dense (cold, intermediate salinity) intermediate and deep waters. The surface waters leave the Nordic Seas via Denmark Strait and enter the subpolar North Atlantic as a narrow and shallow boundary current (about 2 Sv, Sutherland and Pickart, 2008) on the East Greenland shelf and continental slope. The dense waters exit into the subpolar Atlantic in different pathways via the overflows across the Greenland–Scotland Ridge, mainly through Denmark Strait and the Faroe Bank Channel. This exchange is limited by topographic (hydraulic) control and presently the Nordic Seas contribute only about 6 Sv (Quadfasel and Käse, 2007) to the North Atlantic Deep Water.

Direct current measurements over the Greenland–Scotland Ridge show that the Nordic Loop of the Subpolar Gyre of the North Atlantic has a strength of about 8 Sv. Seasonal variability of these exchanges across the ridge is small and amounts to 1 Sv at most (Hansen and Østerhus, 2007). In contrast, the internal horizontal circulation cells in the Nordic Seas that are linked to the four topographic basins are at least twice as strong as the overall exchange, with their seasonal variability exceeding that of the ridge exchanges by an order of magnitude.

The main role of the Nordic gyres thus is the transformation of buoyant surface water into dense deep and intermediate water. This process and the associated circulation set up and maintain fronts. Instabilities of the fronts then provide the energy for meso- and submesoscale stirring and mixing, transferring the transformed water masses from the gyres' interior to the boundary currents. These eventually feed the overflows into the North Atlantic.

7. Acknowledgments

Rolf Käse provided valuable comments on the first draft of this manuscript. The financial support for this study by Deutsche Forschungsgemeinschaft (SFB 512 E2) and the European Commission (Euro-Argo and Mersea) is gratefully acknowledged. These funding agencies also provided most of the Nordic Seas floats. Globally Argo data are collected and made freely available by the International Argo Project and the national programs that contribute to it (http://www.argo.ucsd.edu, http://argo.jcommops.org). Argo is a pilot program of the Global Ocean Observing System.

References

Aagaard, K. and Coachman, L. K. 1968. The East Greenland Current north of Denmark Strait. Part I. *Arctic* **21**(3), 181–200.

Aagaard, K. 1970. Wind-driven transports in the Greenland and Norwegian Seas. *Deep-Sea Res.* **17**, 281–291.

Davis, R. E. 1998. Preliminary results from directly measuring middepth circulation in the tropical and South Pacific. *J. Geophys. Res.* **103**(C11), 24619–24639.

Gascard, J.-C. and Mork, K. A. 2008. Climatic Importance of Large-Scale and Mesoscale Circulation in the Lofoten Basin Deduced from Lagrangian Observations. In: *Arctic-Subarctic Ocean Fluxes*, (eds R. R., Dickson, J., Meincke and P., Rhines), Springer, Dordrecht, 131–143.

Gould, W. J. 2005. From Swallow to Argo—the development of neutrally buoyant floats. *Deep-Sea Res. Part I* **52**, 529–543.

Hansen, B. and Østerhus, S. 2000. North Atlantic-Nordic Seas exchanges. *Prog. Oceanogr.* **45**, 109–208.

Hansen, B. and Østerhus, S. 2007. Faroe Bank Channel Overflow 1995-2005. *Prog. Oceanogr.* **75**, 817–856.

Helland-Hansen, B. and Nansen, F. 1909. The Norwegian Sea: Its Physical Oceanography based on Norwegian Researches. Report on Norwegian Fishery and Marine Investigations 11, 390 pp. + 25 plates.

Holloway, G., Dupont, F., Golubeva, E., Häkkinen, S., Hunke, E. and co-authors. 2007. Water properties and circulation in Arctic Ocean models. *J. Geophys. Res.* **112**(C4), C04S03.

Isachsen, P. E., LaCasce, J. H., Mauritzen, C. and Häkkinen, S. 2003. Wind-driven variability of the large-scale recirculating flow in the Nordic Seas and Arctic Ocean. *J. Phys. Oceanogr.* **33**, 2534–2550.

Jakobsen, P. K., Ribergaard, M. H., Quadfasel, D., Schmith, T. and Hughes, C. W. 2003. Near-surface circulation in the northern North Atlantic as inferred from Lagrangian drifters: variability from the mesoscale to interannual. *J. Geophys. Res.* **108**(C8), 3251.

Jakobsson, M., Cherkis, N., Woodward, J., Coakley, B. and Macnab, R. 2000. New grid of Arctic bathymetry aids scientists and mapmakers. *EOS, Trans. Am. Geophys. Un.* **81**(9), 89.

Jónsson, S. 1991. Seasonal and interannual Variability of Wind Stress Curl Over the Nordic Seas. *J. Geophys. Res.* **96**(C2), 2649–2659.

Kalnay, E., Kanamitsu, M., Kistler, R., Collins, W., Deaven, D. and co-authors. 1996. The NCEP/NCAR 40-Year Reanalysis Project. *B. Am. Meteorol. Soc.* **77**(3), 437–472.

Killworth, P. D. 1992. An equivalent-barotropic mode in the fine resolution antarctic model. *J. Phys. Oceanogr.* **22**, 1379–1387.

Köhl, A. 2007. Generation and stability of a quasi-permanent vortex in the Lofoten Basin. *J. Phys. Oceanogr.* **37**, 2637–2651.

Kolstad, E. W. 2008. A QuikSCAT climatology of ocean surface winds in the Nordic seas: identification of features and comparison with the NCEP/NCAR reanalysis. *J. Geophys. Res.* **113**, D11106.

Lavender, K. V., Owens, W. B. and Davis, R. E. 2005. The mid-depth circulation of the subpolar North Atlantic Ocean as measured by subsurface floats. *Deep-Sea Res. Part I* **52**, 767–785.

Lebedev, K. V., Yoshinari, H., Maximenko, N. A. and Hacker, P. W. 2007. YoMaHa'07: Velocity data assessed from trajectories of Argo floats at parking level and at the sea surface. *IPRC Tech. Rep.* **4**(2), 16 pp.

Machín, F., Send, U. and Zenk, W. 2006. Intercomparing drifts from RAFOS and profiling floats in the deep western boundary current along the Mid-Atlantic Ridge. *Sci. Mar.* **70**(1), 1–8.

Marotzke, J. and Willebrand, J. 1996. The North Atlantic mean circulation: combining data and dynamics. In: *The Warm water sphere of the North Atlantic Ocean* (eds W. Krauss et al.), Borntraeger, Berlin, Stuttgart, 55–90.

Mauritzen, C. 1996. Production of dense overflow waters feeding the North Atlantic across the Greenland-Scotland Ridge. Part 1: evidence for a revised circulation scheme. *Deep-Sea Res. Part I* **43**, 769–806.

Mork, K. A. and Skagseth, Ø. 2005. Annual Sea Surface Height Variability in the Nordic Seas and Arctic Ocean estimated from simplified dynamics. In: *The Nordic Seas: An Integrated Perspective* (eds H. Drange, T. Dokken, T. Furevik, R. Gerdes and W. Berger), Geophys. Monogr. Ser. **158**, AGU, Washington DC, 51–64.

Nøst, O. A. and Isachsen, P. E. 2003. The large-scale time-mean ocean circulation in the Nordic Seas and Arctic Ocean estimated from simplified dynamics. *J. Mar. Res.* **61**, 175–210.

Orvik, K. A. 2004. The deepening of the Atlantic water in the Lofoten Basin of the Norwegian Sea, demonstrated by using an active reduced gravity model. *Geophys. Res. Lett.* **31**, L01306.

Orvik, K. A. and Niiler, P. 2002. Major pathways of Atlantic water in the northern North Atlantic and Nordic Seas toward Arctic. *Geophys. Res. Lett.* **29**, 1986.

Orvik, K. A., Skagseth, Ø. and Mork, M. 2001. Atlantic inflow to the Nordic Seas: current structure and volume fluxes from moored current meters, VM-ADCP and SeaSoar-CTD observations, 1995–1999. *Deep-Sea Res. Part I* **48**, 937–957.

Park, J. J., Kim, K., King, B. A. and Riser, S. 2005. An advanced method to estimate deep currents from profiling floats. *J. Atmos. Ocean. Tech.* **22**, 1294–1304.

Poulain, P.-M., Warn-Varnas, A. and Niiler, P. P. 1996. Near-surface circulation of the Nordic seas as measured by Lagrangian drifters. *J. Geophys. Res.* **101**(C8), 18237–18258.

Quadfasel, D. and Käse, R. 2007. Present-Day Manifestation of the Nordic Seas Overflows. In: *Ocean Circulation: Mechanisms and Impacts* (eds A. Schmittner, J. C. H. Chiang and S. R. Hemmings), Geophys. Monogr. Ser. **173**, AGU, Washington DC, 75–89.

Roemmich, D., Boebel, O., Desaubies, Y., Freeland, H., Kim, K. and co-authors. 1999. Argo: the global array of profiling floats. In: *Observing the Oceans in the 21st Century* (eds C. J. Koblinsky and N. R. Smith), GODAE Project Office and Bureau of Meteorology, Melbourne, 248–257.

Rossby, T., Prater, M. D. and Søiland, H. 2009. Pathways of inflow and dispersion of warm waters in the Nordic seas. *J. Geophys. Res.* **114**, C04011.

Serra, N., Käse, R. H., Köhl, A., Stammer, D. and Quadfasel, D. 2010. On the low-frequency phase relation between the Denmark Strait and the Faroe-Bank Channel overflows. *Tellus* **62A**.

Smith, W. H. F. and Sandwell, D. T. 1997. Global sea floor topography from satellite altimetry and ship depth soundings. *Science* **277**, 1956–1962.

Søiland, H., Prater, M. D. and Rossby, T. 2008. Rigid topographic control of currents in the Nordic Seas. *Geophys. Res. Lett.* **35**, L18607.

Sutherland, D. A. and Pickart, R. S. 2008. The east Greenland coastal current: structure, variability, and forcing. *Prog. Oceanogr.* **78**, 58–77.

Thomson, R. E. and Freeland, H. J. 2003. Topographic steering of a mid-depth drifter in an eddy-like circulation region south and east of the Hawaiian Ridge. *J. Geophys. Res.* **108**(C11), 3341.

Woodgate, R. A., Fahrbach, E. and Rohardt, G. 1999. Structure and transports of the East Greenland Current at 75°N from moored current meters. *J. Geophys. Res.* **104**(C8), 18059–18072.